Changes in growth kinetics of stamen filaments cause inefficient pollination in *massugu2*, an auxin insensitive, dominant mutant of *Arabidopsis thaliana*

Satoko Tashiro,[a] Chang-en Tian,[b,†] Masaaki K. Watahiki[a, b,*] and Kotaro T. Yamamoto[a, b]

[a] Biosystems Science Course, Gradate School of Life Science, Hokkaido University, Sapporo, 060-0810 Japan

[b] Department of Biological Sciences, Faculty of Science, Hokkaido University, Sapporo, 060-0810 Japan

[†] Present address: School of Life Science, Guangzhou University, 230# Waihuanxi Road, Guangzhou Higher Education Mega Center, Guangzhou 510006, China

Abstract

We investigated the physiological and molecular basis of lower fecundity of *massugu2* (*msg2*), which is a dominant mutant of an auxin primary response gene, *IAA19*, in *Arabidopsis thaliana*. By measuring the length of all stamens and pistils in inflorescences and the reference growth rate of pistils, we constructed growth curves of pistils and stamens between stages 12 and 15 of flower development. Pistil growth was found to consist of a single exponential growth, while stamen growth consisted of three exponential phases. During the second exponential phase, the growth rate of stamen filaments was ~10 times greater than the growth rates in the other two

phases. Consequently, stamens whose growth was initially retarded grew longer than the pistil, putting pollen grains on the stigma. *msg2-1* stamens, on the other hand, exhibited a less obvious growth increase, resulting in less frequent contact between anthers and stigma. *MSG2* was expressed in the stamen filaments and its expression almost coincided with the second growth phase. Stamen filaments appeared to elongate by cell elongation rather than cell division in the epidermal cell file. Considering that MSG2 is likely to be a direct target of the auxin F-box receptors, *MSG2* may be one of the master genes that control the transient growth increase of stamen filaments.

Abbreviations -- GUS, β-glucuronidase; NAA, 1-naphthaleneacetic acid; RT-PCR, reverse transcription-polymerase chain reaction.

Introduction

Auxin is known to affect several distinct processes needed for full development of fecundity in the autogamous plant *Arabidopsis thaliana*. First, auxin is needed for organogenesis of floral organs in the early stages of flower development; disruption of either polar auxin transport (Okada et al. 1991, Nemhauser et al. 2000) or auxin biosynthesis (Cheng et al. 2006) causes various severe defects in flower formation. Second, flower development is arrested in the middle of flower development in an auxin-signaling mutant such as the *auxin response factor6* (*arf6*) and *arf8* double mutant. Thus, auxin regulates the transition from immature to

mature fertile flowers (Nagpal et al. 2005, Wu et al. 2006). This transition is found to be accomplished partially through jasmonic acid which could function under the control of auxin (Ishiguro et al. 2001, Nagpal et al. 2005). Third, at a later stage of flower development, the elongation of the stamen is retarded relative to that of the pistil in some auxin-signaling and transport mutants, resulting in inefficient pollination in spite of normal development of reproductive organs (Noh et al. 2001, del Pozo et al. 2002). This indicates that coordinated elongation between the stamen filament and pistil is required for self-pollination (Nagpal et al. 2005, Cecchetti et al. 2008).

The *massugu2* (*msg2*) mutant was identified as a mutant of which hypocotyl did not bend upon unilateral application of auxin. *msg2* is caused by a dominant mutation in one of *Aux/IAA* genes, *IAA19* (Tatematsu et al. 2004). Aux/IAA proteins are thought to function directly under the control of auxin F-box receptors to regulate transcriptional activities of downstream ARFs (Tan et al. 2007, Benjamins and Scheres 2008). The *msg2* defects include lower fecundity as well as abnormalities in tropic responses and lateral root formation (Tatematsu et al. 2004). Here, we investigated the physiological and molecular basis of lower fecundity of *msg2*, and found that *msg2* infertility belonged to the third category of auxin-involved infertility mentioned above. Arabidopsis fecundity has often been shown to require concerted growth between the pistil and stamens (Nagpal et al. 2005, Cecchetti et al. 2008). Therefore, we examined it in a more quantitative manner in this study. Measurement of length of all the pistils and stamens in many inflorescences allowed us to construct growth curves of the two floral organs. We also investigated the expression of *MSG2* in stamen filaments. Our results suggest that *MSG2/IAA19* is one of the master genes

that regulate elongation of stamen filaments.

Materials and methods

Plant materials and growth conditions

All the mutants of *Arabidopsis thaliana* were Columbia (Col) background except for *msg2-21* (Tatematsu et al. 2004), *arf8-1* (Tian et al. 2004) and *arf6-101* which were Wassilewskija (Ws) background. *arf6-101* (FLAG219_A05) was identified from the FLAG_FST collection (Samson et al. 2002). Plants were grown on a 1:1 (v/v) mixture of vermiculite and Metromix 350 (Scotts-Sierra, Marysville, Ohio, USA) at 23°C under continuous illumination at a fluence rate of 14 W m^{-2} obtained from two 40-W white fluorescent tubes (FL40SW; NEC Lighting, Tokyo, Japan) and one 40-W blue and red-enhanced fluorescent tube (FL40SBR-HG, NEC Lighting).

Measurement of length of flower organs

Inflorescences were fixed in 70% ethanol, which also removed pigments. Then, images of flowers were taken with a dissecting microscope (MZ12, Leica, Nubloh, Germany) equipped with a digital camera (DXM1200, Nikon, Tokyo, Japan) after immersion in clearing solution (chloral hydrate : glycerol : water = 100 g : 10 g : 25 ml). Stamen and pistil length was measured in images using ImageJ software (NIH, Bethesda, Maryland, USA). Stamen length was determined as the distance from the base of the stamen filament to the tip of the anther. Pistil length was determined as

the distance from the base of the pistil to the base of the stigma papillae.

Auxin treatment and histochemical β-glucuronidase (GUS) staining

The *MSG2* promoter::*GUS* line (*pMSG2::GUS*) was described in Tatematsu et al. (2004). After each flower bud was gently broken by poking with the tip of the knife blade, 3 to 4 inflorescences were put in 1 ml of 50 mM sodium phosphate, pH 7.0, and 0.1% Tween 20 with or without 50 μM 1-naphthaleneacetic acid (NAA), subjected to weak vacuum for ~10 s, and incubated at 23°C for 2 h in the light. Inflorescences were then fixed with ice-cold 50% acetone for 30 min, rinsed with 50 mM sodium phosphate, pH 7.0, for three times on ice. They were stained with 50 mM sodium phosphate, pH 7.0, containing 2 mM 5-bromo-4-chloro-3-indolyl-β-D-glucuronide (X-Gluc), 5 mM $K_3Fe(CN)_6$, 5 mM $K_4Fe(CN)_6$, 1 mM EDTA and 0.1% Tween 20 for 24 h at 23°C, and treated with 70% ethanol to remove pigments. For staining of the *DR5::GUS* line (Sabatini et al. 1999), X-Gluc was used in the concentration of 4 mM. After immersion in the clearing solution for ~24 h, images of the stained flowers were taken with the above-mentioned dissecting microscope, and were RGB-split, using ImageJ software. Because blue color was shown as black in the 'red' image, intensity of GUS staining was determined as a maximum value of the most stained area of each stamen filament in the 'red' image. Background level was determined in flowers stained in the absence of X-Gluc.

Quantitative reverse transcription-polymerase chain reaction (RT-PCR) analysis

Quantitative RT-PCR was carried out essentially in the same way as described by Sato and Yamamoto (2008). Total RNA was extracted from flowers or flower buds using an RNeasy Plant Mini Kit (Qiagen, Hilden, Germany), and reverse-transcribed using a QuantiTect Reverse Transcription Kit (Qiagen). Quantitative real-time PCR was performed with a LightCycler 480 II/96 (Roche, Basel, Switzerland) and SYBER-Green PCR Master Kit (Applied Biosystems, Foster City, California, USA). Each PCR reaction was made in triplicate. Expression levels of *MSG2* were normalized to the levels of *ACTIN2*. The efficiency of PCR was determined in each 96-well plate by measuring PCR reactions of cDNA samples serially diluted with reverse-transcribed mock RNA samples. The PCR primers for *MSG2* cDNA were 5'-ATCGGTGTGGCCTTGAAAGA -3' and 5'-AACATCCCCCAAGGTACATCAC-3'. *ACTIN2* primers were 5'-CGCTCTTTCTTTCCAAGCTCATA-3' and 5'-CCATACCGGTACCATTGTCACA-3'.

Results

Lower fecundity of the *msg2* mutants

Mature *msg2-1* plants were previously found to be similar in size and morphology to wild type (Col ecotype) except for their lower fecundity (Tatematsu et al. 2004). Since the *msg2-1* fecundity was improved in older plants, we examined plants that were younger than 8 weeks old. Most of wild-type fruits had 40 - 60 seeds (Fig. 1A), while *msg2-1* fruits possessed

less than 10 seeds (Fig. 1B). But, they contained as many seeds as wild-type fruits when *msg2-1* flowers were manually self-pollinated (Fig. 1C). These results show that the reduced fecundity of *msg2-1* is due to inefficient pollination rather than defects in formation of gametes.

Relationship between the elongation of the pistil and stamens

We observed development of flower organs to determine the physiological and molecular basis of reduced fecundity in *msg2-1*. In a wild-type flower, anthers deposit pollen grains on stigma papillae when stamens extend above the pistil at stage 14 of flower development (Smyth et al. 1990). In contrast, most stamens in *msg2-1* flowers did not exceed the height of the pistil and failed in pollinating (Fig. 2A). To further investigate this difference in a quantitative manner, we measured the lengths of the pistil and the four long stamens and the two short stamens in each flower of an inflorescence in which the pistil was longer than 1.0 mm. A flower with a 1.0-mm-long pistil corresponds to a flower at stage 12, the final bud stage. The length of the stamens is plotted as a function of the length of the pistil in each flower in Fig. 2B (top). The stamens that are longer than the pistil are located above the thin line that has a slope of 45° and passes through the origin in this figure. In the wild type, 51% of the long stamens were longer than the pistil, whose length was between 1.8 and 2.1 mm (Fig. 2B, top left), while only 2.5% of the long stamens exceeded above the pistil in *msg2-1* (Fig. 2B, top right). This difference is likely to cause inefficient pollination in *msg2-1*. The short stamens were always shorter than the long stamens by ~25% so that no short stamens grew longer than the pistil. This suggests that the short

stamens contribute little or nothing to pollination. *msg2-21* is a T-DNA insertion line, and was thought to be a loss-of-function mutant of *MSG2* because no *MSG2* mRNA was detectable in an RNA blot analysis (Tatematsu et al., 2004). The relationship between the lengths of the pistil and the stamens of *msg2-21* was essentially the same as that in the wild type Ws (Suppl. Fig. 1), which was consistent with normal fecundity of msg*2-21* (data not shown).

Population structure and growth kinetics of pistil and stamen

We investigated the population structure of pistils longer than 1.0 mm and the long and short stamens longer than 0.7 mm with respect to their length (Fig. 2B bottom and Fig. 3, respectively). The relative frequency of pistils or stamens in a given class is proportional to the time duration during which a pistil or a stamen grows from the lower end point to the upper end point of the class, if production of flowers is in the steady state. We examined growth of flower organs of ~7-week-old plants, where flowers were continually produced. Thus, the growth rate of the pistil or stamen is inversely proportional to the relative frequency (note that the class interval is constant, 0.1 mm). The results show that the relative frequency of pistil length decreased almost monotonously as pistil length increased in the wild type (Fig. 2, bottom left), while the relative frequency of the long stamens had a minimum in the length class of 1.6 – 1.7 mm irrespective to genotype (Fig. 3, top). The population structure of the short stamen was very similar to that of the long stamen, except that the distribution shifted to shorter lengths by 0.3 - 0.4 mm (Fig. 3, bottom).

Because population structure of pistil and stamen is directly related to their relative growth rate, we can construct their absolute growth curves if a reference growth rate is available. We removed a sepal from a flower, and determined the length of the exposed pistil at several time points. These experiments showed that the time needed for pistils to elongate from 1.5 to 2.5 mm was 36.8 ± 7.0 h (n = 18) for the wild type and 39.7 ± 6.8 h (n = 20) for *msg2-1*. The mean growth rates of pistils were 0.028 ± 0.006 and 0.026 ± 0.005 mm/h in the wild type and *msg2-1*, respectively. When the pistil was 1.5 and 2.5-mm long, the long stamens were 1.06 and 2.21-mm long, respectively, in the wild type (Fig. 2B, top left), and 0.962 and 2.16-mm long, respectively, in *msg2-1* (Fig. 2B, top right). The growth curves in Fig. 4 (top and middle) were constructed using these reference values and the data in Figs. 2B and 3, and the growth rates in Fig. 4 (bottom) were calculated from the growth curves. These analyses showed several characteristics of the pistil and stamen growth. Growth of the wild-type pistil was approximated as a single exponential growth up to a length of 2.7 mm ($t \leqq 69.1$ h; Fig. 4, middle left). The increase in pistil growth rate that resulted in deviation from the exponential growth after 69.1 h was likely to be due to the development of the pistil into a silique after pollination. On the other hand, growth of the *msg2-1* pistil remained exponential for a longer time than that of the wild type (Fig. 4, middle right), which may be indicative of infrequent pollination of *msg2-1*. In contrast to the pistil growth, growth of the long stamens consisted of three exponential growth phases (Fig. 4, middle left). The second exponential phase was the fastest growing phase of the three, during which the long stamens caught up with the pistil and

extended above it. Growth of the *msg2-1* long stamens also consisted of the three growth phases (Fig. 4, middle right). However, the second phase was less prominent in *msg2-1*, and occurred later than that of the wild type by ~8 h. The highest growth rate observed in the second growth phase was ~11 times higher than the background level in the wild type, while it was ~7 times higher in *msg2-1* (Fig. 4, bottom). The *msg2-1* stamens also elongated more than the wild-type stamens (Fig. 3, top), which likely reflects the slower senescence of the mutant stamens due to infrequent pollination.

MSG2 gene expression along elongation of stamen filament

To examine the expression domain of *MSG2* gene in flower, we performed histochemical GUS staining of the upper part of inflorescences of the *MSG2* promoter::*GUS* (*pMSG2::GUS*) plants (Tatematsu et al. 2004). Results in Fig. 5A and B show that *MSG2* expression was almost restricted to the elongated filaments of the stamens. Nectars and anthers were sometimes stained faintly (Fig. 5A). In order to estimate *MSG2* expression activity in a more quantitative manner, we measured the intensity of blue color of the GUS reaction product in the filaments as a function of stamen length. We also carried out the same experiments after inflorescences were treated with 50 μM NAA for 2 h to know the effects of exogenously applied auxin on *MSG2* expression in the filaments. These measurements summarized in Fig. 5C (top) for the long stamens show that *MSG2* started to be expressed significantly ($P = 0.028$; Student's *t*-test) when the long stamens reached a length of 1.4 - 1.5 mm. Then, *MSG2* expression increased rapidly and reached a plateau at ~2.1 mm. It was further increased upon auxin

treatment only when stamens were longer than 1.8 mm. But the maximum expression level seemed to be unaffected by auxin treatment.

We also examined the activity of the auxin-responsive, synthetic promoter, *DR5*, using the *DR5::GUS* plants (Sabatini et al. 1999). Because only anthers were stained in our experimental condition, we measured the intensity of blue color in the anthers as a function of stamen length (Fig. 5C, bottom). *DR5* activity of the anthers was highest in the 0.5 – 0.6-mm long stamens. It then decreased as the stamens elongated, and no significant signal was observed when the stamens were longer than 0.9 mm. However, large standard deviations at ~1.5 mm reflected sporadic GUS signals in the anthers.

MSG2 gene expression revealed with quantitative RT-PCR

We measured the *MSG2* expression levels in wild-type and *msg2-1* flowers from stage 12 to 15 with quantitative RT-PCR (Fig. 6). Stage 12 is the final bud stage, and we examined growth of pistils and stamens from this stage. Stage 13 begins when flower buds open; the long stamens extend above the stigma at stage 14, and the stigma extends again above the long stamens at stage 15 (Smyth et al., 1990). In both the wild type and *msg2-1*, stage 13 and 14 flowers contained higher levels of *MSG2* mRNA than stage 12 flowers ($P < 0.05$ in *t*-test). However, the stage-specific increase in the *MSG2* mRNA level was more prominent in the wild type than in *msg2-1*.

Cell number of an epidermal cell file of the stamen filament

The stamen filament elongates rapidly throughout flower development.

The growth may result from an increase in cell division, cell elongation or both. We counted the number of cells of an epidermal cell file in stamen filaments of various lengths to see which was the most important factor in elongation growth of stamen filament. The results in Fig. 7 show that regardless of the length of the filaments, the cell number of the longitudinal cell files was almost constant both in the wild type and *msg2-1*: the long stamens had ~26 cells, and the short stamens had ~20 cells. This indicates that elongation of stamen filament is caused by an increase in cell elongation. In addition, the difference of length of the long and the short stamen appears to be due to a difference in cell number.

Relationship between pistil and stamen growth in auxin signaling mutants

Aux/IAAs are thought to act by inhibiting function of target ARFs. MSG2 is likely to act with NPH4/ARF7 and ARF19 in tropic responses of hypocotyl and lateral root formation (Tatematsu et al. 2004, Okushima et al. 2005b). Therefore, we examined the relationship between elongation of pistils and stamens in flowers of the *nph4-1* and *arf19-1* single mutants (see Appendix S1 in Supporting Information) and their double mutant (Fig. 8F). Both mutants exhibited a normal relationship, confirming a previous report that *nph4-1 arf19-1* bears normal flowers and exhibits wild-type fecundity (Okushima et al. 2005b). This suggests that other ARFs are involved in the concerted elongation of stamens and pistils. Because defects in stamen elongation had been described in *arf6* and *arf8* mutants (Nagpal et al. 2005), we measured *arf6-101* (Fig. 8C) and *arf8-1* flowers (Fig. 8D), and found that they showed defects in the pistil-stamen relationship although the defects

were weaker than the defect in *msg2-1*. We also examined flowers of other dominant mutants of *Aux/IAA*. *axr3-1/iaa17* (Rouse et al. 1998) showed similar defects to *msg2-1/iaa19* (Fig. 8B), while *axr2-1/iaa7* (Nagpal et al. 2000) and *slr-1/iaa14* (Fukaki et al., 2006) were normal (see Appendix S1 in Supporting Information). Both *AXR3* and *AXR2* are expressed in flowers with a peak at stage 13 – 14 in the *ARF6* and *ARF8*-dependent manner (Nagpal et al. 2005). Although expression of one of the polar auxin transport facilitator genes, *PIN3*, also increases in the stamens as the flower develops (Mandaokar et al., 2006), the pistil-stamen relationships of *pin3-4* and *pin3-5* mutants were not affected (see Appendix S1 in Supporting Information).

Discussion

Growth curves of pistils and stamens at the later stages of Arabidopsis flower development (stages 12 - 15) were constructed in the present study by examining all the flowers in inflorescences and using the growth rate of the pistil as a reference. The results show that pistil growth is formed from a single exponential growth. On the other hand, stamen growth consists of three exponential growth phases, and the long stamens catch up with the pistil in the second growth phase. In the case of *Lilium longiflorum,* the elongation of both pistils (Crone and Lord 1991) and filaments (Erickson 1948) has been shown to be exponential until anthesis. Since the anthers of Arabidopsis have almost reached their mature length at stage 12 (Smyth et al. 1990), the elongation of stamens described in this study is mostly due to

the elongation of the stamen filament. We also show that the filaments elongate by cell elongation rather than by cell division in the epidermal cell file (Fig. 6), as is the case with hypocotyl elongation in Arabidopsis (Gendreau et al. 1997). The same results were reported in filaments of *Ipomoea nil* (Koning and Raab 1987) and *Gaillardia grandiflora* (Koning 1983). In the case of *Cleome hassleriana* (Koevenig 1973) and *Nigella hispanica* (Greyson and Tepfer 1966), filament elongation at the later stages of flower development appears to be due to cell elongation based on the elongation of epidermal cells.

In the wild type, the growth rate of stamens in the catch-up phase of stamen growth is more than 10 times greater than the growth rates in the first and the third exponential growth phases. In *msg2*, however, the growth rate in the catch-up phase does not increase so much, resulting in less frequent contact between stamens and the pistil, and thus lower fecundity. According to the activity of *MSG2 promoter GUS*, *MSG2* expression in stamen filaments starts to increase at a stamen legth of 1.4 – 1.5 mm, and reaches a plateau at a stamen length of 2.1 - 2.2 mm (Fig. 5C). This period of expression well coincides with the second exponential phase, suggesting that MSG2 is involved in the rapid elongation at this time. In view of the findings that MSG2/IAA19 is possibly a direct target of auxin F-box receptors (AFB; Tan et al. 2007), and that AFB-deficient mutants, like the *msg2* mutant, are defective in stamen elongation (Cecchetti et al. 2008), *MSG2* may be one of the master genes that regulate elongation of stamen filaments in the catch-up phase. On the other hand, a loss-of-function mutant of *MSG2* (*msg2-21*) did show the wild-type phenotype in the growth relationship between pistils and stamens (see Appendix S1 in Supporting

Information), and exhibited normal fecundity. In fact, no aberrant phenotype has been observed in *msg2-21* so far (Tatematsu et al., 2004). Closely-related Aux/IAAs such as IAA5 and IAA6 may possibly replace MSG2 function in *msg2-21*.

We previously pointed out that *MSG2* could be one of the master genes for tropic responses in hypocotyls (Saito et al. 2007). It is noteworthy that the role of *MSG2* in phototropic bending of light-grown hypocotyl parallels its role in the catch-up phase of stamen elongation. As mentioned above, the Arabidopsis hypocotyl elongates solely by cell elongation in the epidermal cell file (Gendreau et al. 1997). During phototropic bending, *MSG2* is expressed on the convex side of the hypocotyl only in the bending phase and thereafter when monitored with the same *MSG2 promoter::GUS* line. During the basal growth phase before exposure to phototropic stimuli, *MSG2* expression is not observed. Thus, MSG2 appears to be an auxin-dependent mediator specific for transient growth responses.

The *msg2* mutant was identified as a mutant whose hypocotyl did not bend upon unilateral application of auxin to the hypocotyl (Tatematsu et al. 2004). The same screening procedure identified another bending-defective mutant, *msg1/nph4* (Watahiki and Yamamoto 1996). *msg2* harbors a dominant mutation in one of the *Aux/IAA* genes, *IAA19* (Tatematsu et al. 2004), while *nph4* is a recessive mutant of *ARF7* (Harper et al. 2000). Disruption of *ARF19*, which is most closely related to *NPH4* in the *ARF* family, generally enhances defects in *nph4*, indicating that the two genes have overlapping roles (Okushima et al. 2005b, Wilmoth et al. 2005). Though the hypocotyls of *msg2* and *nph4* mutants exhibit reduced gravitropic or phototropic curvature, *msg2* defects are more severe than

those of *nph4* (Tatematsu et al. 2004). Thus, according to the current model of auxin signaling (Benjamins and Scheres 2008), MSG2 is thought to regulate the bending responses just downstream of the auxin F-box receptors by inhibiting transcriptional activity of NPH4 and ARF19. In the case of elongation of stamen filaments in this study, however, both *nph4* and *arf19* single mutants and their double mutant exhibited a normal growth relationship between the pistil and stamens (Fig. 8F), even though both *NPH4* and *ARF19* are expressed in stamen filaments (Wilmoth et al. 2005). This clearly indicates that neither gene is a target of *MSG2*. Instead, loss-of-function mutants of *ARF6* and its most closely-related gene, *ARF8*, showed weaker defects than *msg2* (Fig. 8C and D). Considering that both genes are expressed in stamen filaments strongly (Nagpal et al. 2005, Goetz et al. 2006, Wu et al. 2006), *ARF6* and *ARF8* appear to be target genes of *MSG2* in regulation of stamen elongation.

Flower development of the *arf6-2 arf8-3* double mutant is arrested at stage 12, producing infertile closed buds (Nagpal et al. 2005). Apparently the catch-up phase of stamen elongation disappears in the double mutant. A double mutant of our alleles, *arf6-101* and *arf8-1*, also displayed essentially the same defects in flower development (our unpublished data). According to the growth data of Nagpal et al. (2005), stamen elongation may be inhibited also in the first exponential growth phase in *arf6-2 arf8-3*. A loss-of-function mutant of another ARF, ARF2, also has flowers whose stamens are shorter than the pistil in the early phase of reproductive development (Ellis et al. 2005, Okushima et al. 2005a, Schruff et al. 2006). ARF2 acts as a transcriptional repressor in vitro in contrast to ARF6 to 8 which function as activators (Tiwari et al. 2003). Furthermore, global

transcriptome analyses have not lead to consistent understanding of ARF2's role in auxin-induced gene expression, and even a possibility that ARF2 may not conform to the canonical auxin response model is suggested (Ellis et al. 2005, Okushima et al. 2005a).

MSG2/IAA19 is thought to be a primary auxin-responsive gene (Tatematsu et al. 2004). Microarray analyses of Arabidopsis flowers at different stages show that *MSG2* is one of 911 genes whose expression peaks at stage 13 – 14; *MSG2* expression is also dependent on *ARF6* and *ARF8* (Nagpal et al. 2005). We showed here that brief application of auxin increased the expression of *MSG2* in stamen filaments in the late catch-up phase and thereafter. However, *MSG2* was not expressed in stamen filaments even after NAA application in the first exponential growth phase (Fig. 5C), indicating that auxin is not the rate-limiting factor for *MSG2* expression in this developmental phase. This highlights the importance of developmental stage-specific factors that are needed for expression of *MSG2*. Identification of these factors is essential for understanding the molecular mechanism of concerted growth of floral organs.

Microarray data show that the increase in *MSG2* expression during flower development parallels increases in the expressions of the polar auxin transport facilitators, PIN3, PIN4 (Nagpal et al. 2005) and PIN8 (Mandaokar et al. 2006). This suggests that *MSG2* expression is induced by the polarly transported auxin in the catch-up phase. Free auxin is accumulated in anthers at stages 10 - 12, as judged by the expression of the *DR5::GUS* reporter gene (Aloni et al. 2006, Feng et al. 2006, Cecchetti et al. 2008). But the auxin level in the anthers decreases to the background level in the catch-up phase (Fig. 5C, bottom; Cecchetti et al. 2008). Auxin was

detected at the tip of the stamen filaments in the later developmental stages (Aloni et al. 2006). This may be the source of auxin that induces the expression of *MSG2*.

Finally we have to ask what kind of molecules control elongation in the first exponential growth phase of stamen elongation. Pistil growth and the first growth phase of the stamens are characterized by a single exponential growth (Fig. 4B), suggesting that the growth of both pistils and stamens is regulated by a common regulatory pathway. Candidate molecules that control their growth would be gibberellin and brassinosteroid. Both gibberellin (Goto and Pharis 1999) and brassinosteroid (Catterou et al. 2001)-deficient mutants form pistils and stamens that are shorter than those of the wild type.

Acknowledgements -- The authors thank Dr. T. M. Guilfoyle for the *DR5::GUS* line, Dr. E. Liscum for *nph4-1*, Dr. M. Tasaka for *slr*, Arabidopsis Biological Resource Center for *axr1*, *axr2*, *axr3*, *arf19* and *pin3*, and *Arabidopsis thaliana* Resource Centre for Genomics/INRA for *arf6*. C.-e.T. was supported by Postdoctoral Fellowship of Japan Society of Promotion of Science. This work was supported in part by a Grant-in-Aid for Scientific Research in Priority Areas from the Ministry of Education, Culture, Sports, Science and Technology to K.T.Y. (#19060008).

References

Aloni R, Aloni E, Langhans M, Ullrich CI (2006) Role of auxin in regulating *Arabidopsis* flower development. Planta 223: 315-328

Benjamins R, Scheres B (2008) Auxin: The looping star in plant development. Annu Rev Plant Biol 59: 443-465

Catterou M, Dubois F, Schaller H, Aubanelle L, Vilcot B, Sangwan-Norreel BS, Sangwan RS (2001) Brassinosteroids, microtubules and cell elongation in *Arabidopsis thaliana*. I. Molecular, cellular and physiological characterization of the *Arabidopsis bul1* mutant, defective in the Δ^7-sterol-C5-desaturation step leading to brassinosteroid biosynthesis. Planta 212: 659-672

CecchettiV, Altamura MM, Falasca G, Costantino P, Cardarellic M (2008) Auxin regulates *Arabidopsis* anther dehiscence, pollen maturation, and filament elongation. Plant Cell 20: 1760-1774

Cheng Y, Dai X, Zhao Y (2006) Auxin biosynthesis by the YUCCA flavin monooxygenases controls the formation of floral organs and vascular tissues in Arabidopsis. Genes Dev 20: 1790-1799

Crone W, Lord EM (1991) A kinematic analysis of gynoecial growth in *Lilium longiflorum*: Surface growth patterns in all floral organs are triphasic. Developmental Biol 143: 408-417

del Pozo JC, Dharmasiri S, Hellmann H, Walker L, Gray WM, Estelle M (2002) AXR1-ECR1-dependent conjugation of RUB1 to the Arabidopsis cullin AtCUL1 is required for auxin response. Plant Cell 14: 421-433

Ellis CM, Nagpal P, Young JC, Hagen G, Guilfoyle TJ, Reed JW (2005) *AUXIN RESPONSE FACTOR1* and *AUXIN RESPONSE FACTOR2* regulate senescence and floral organ abscission in *Arabidopsis thaliana*. Development 132: 4563-4574

Erickson RO (1948) Cytological and growth correlations in the flower bud and anther of *Lilium longiflorum*. Amer J Bot 35: 729-739

Fei H, Sawhney VK (1999) Role of plant growth substances in *MS33*-controlled stamen filament growth in *Arabidopsis*. Physiol Plant 105: 165-170

Feng X-L, Ni1 W-M, Elge S, Mueller-Roeber B, Xu Z-H, Xue H-W (2006) Auxin flow in anther filaments is critical for pollen grain development through regulating pollen mitosis. Plant Mol Biol 61: 215-226

Fukaki H, Taniguchi N, Tasaka M (2006) PICKLE is required for SOLITARY-ROOT/IAA14-mediated repression of ARF7 and ARF19 activity during Arabidopsis lateral root initiation. Plant J 48: 380-389

Gendreau E, Traas J, Desnos T, Grandjean O, Caboche M, Höfte H (1997) Cellular basis of hypocotyl growth in *Arabidopsis thaliana*. Plant Physiol 114: 295-305

Goetz M, Vivian-Smith A, Johnson SD, Koltunow AM (2006) *AUXIN RESPONSE FACTOR8* is a negative regulator of fruit initiation in *Arabidopsis*. Plant Cell 18: 1873-1886

Goto N, Pharis RP (1999) Role of gibberellins in the development of floral organs of the gibberellin-deficient mutant, *ga1-1*, of *Arabidopsis thalinana*. Can J Bot 77: 944-954

Greyson RI, Tepfer SS (1966) An analysis of stamen filament growth of

Nigella hispanica. Amer J Bot 53: 485-490

Harper RM, Stowe-Evans EL, Luesse DR, Muto H, Tatematsu K, Watahiki MK, Yamamoto K, Liscum E (2000) The *NPH4* locus encodes the auxin response factor ARF7, a conditional regulator of differential growth in aerial Arabidopsis tissue. Plant Cell 12: 757-770

Ishiguro S, Kawai-Oda A, Ueda J, Nishida I, Okada K (2001) The *DEFECTIVE IN ANTHER DEHISCENCE1* gene encodes a novel phospholipase A1 catalyzing the initial step of jasmonic acid biosynthesis, which synchronizes pollen maturation, anther dehiscence, and flower opening in Arabidopsis. Plant Cell 13: 2191-2209

Koevenig JL (1973) Floral development and stamen filament elongation in Cleome hassleriana. Amer J Bot 60: 122-129

Koning RE (1983) The role of auxin, ethylene, and acid growth in filament elongation in Gaillardia grandiflora (Asteraceae). Amer J Bot 70: 602–610

Koning RE, Raab MM (1987) Parameters of filament elongation in Ipomoea nil (Convolvulaceae). Amer J Bot 74: 510–516

Mandaokar A, Thines B, Shin B, Lange BM, Choi G, Koo YJ, Yoo YJ, Choi YD, Choi G, Browse J (2006) Transcriptional regulators of stamen development in Arabidopsis identified by transcriptional profiling. Plant J 46: 984-1008

Nagpal P, Ellis CM, Weber H, Ploense SE, Barkawi LS, Guilfoyle TJ, Hagen G, Alonso JM, Cohen JD, Farmer EE, Ecker JR, Reed JW (2005) Auxin response factors ARF6 and ARF8 promote jasmonic acid production and flower maturation. Development 132: 4107-4118

Nagpal P, Walker LM, Young JC, Sonawala A, Timpte C, Estelle M, Reed JW

(2000) *AXR2* encodes a member of the Aux/IAA protein family. Plant Physiol 123: 563-573

Nemhauser JL, Feldman LJ, Zambryski PC (2000) Auxin and *ETTIN* in *Arabidopsis* gynoecium morphogenesis. Development 127: 3877-3888.

Noh, B., A. S. Murphy, and E. P. Spalding. 2001. *Multidrug Resistance*-like genes of Arabidopsis required for auxin transport and auxin-mediated development. Plant Cell 13: 2441-2454

Okada K, Ueda J, Komaki MK, Bell CJ, Shimura Y (1991) Requirement of the auxin polar transport system in early stages of *Arabidopsis* floral bud formation. Plant Cell 3: 677-684

Okushima Y, Mitina I, Quach HL, Theologis A (2005a) AUXIN RESPONSE FACTOR 2 (ARF2): a pleiotropic developmental regulator. Plant J 43: 29-46

Okushima Y, Overvoorde PJ, Arima K, Alonso JM, Chan A, Chang C, Ecker JR, Hughes B, Lui A, Nguyen D, Onodera C, Quach H, Smith A, Yu G, Theologis A (2005b) Functional genomic analysis of the *AUXIN RESPONSE FACTOR* gene family members in *Arabidopsis thaliana*: Unique and overlapping functions of *ARF7* and *ARF19*. Plant Cell 17: 444-463

Rouse D, Mackay P, Stirnberg P, Estelle M, Leyser O (1998) Changes in auxin response from mutations in an AUX/IAA gene. Science 279: 1371-1373

Sabatini S, Beis D, Wolkenfelt H, Murfett J, Guilfoyle T, Malamy J, Benfey P, Leyser O, Bechtold N, Weisbeek P, Scheres B (1999) An auxin-dependent distal organizer of pattern and polarity in the Arabidopsis root. Cell 99:

463–472

Saito K, Watahiki MK, Yamamoto KT (2007) Differential expression of the auxin primary-response gene *MASSUGU2/IAA19* during tropic responses of Arabidopsis hypocotyls. Physiol Plant 130: 148-156

Samson F, Brunaud V, Balzergue S, Dubreucq B, Lepiniec L, Pelletier G, Caboche M, Lecharny A (2002) FLAGdb/FST: a database of mapped flanking insertion sites (FSTs) of *Arabidopsis thaliana* T-DNA transformants. Nucleic Acids Res 30: 94-97

Sato A, Yamamoto KT (2008) Overexpression of the noncanonical *Aux/IAA* genes causes auxin-related aberrant phenotypes in Arabidopsis. Physiol Plant 133: 397-405

Schruff MC, Spielman M, Tiwari S, Adams S, Fenby N, Scott RJ (2006) The *AUXIN RESPONSE FACTOR 2* gene of *Arabidopsis* links auxin signalling, cell division, and the size of seeds and other organs. Development 133: 251-261

Smyth DR, Bowman JL, Meyerowitz EM (1990) Early flower development in *Arabidopsis*. Plant Cell 2: 755-767

Tan X, Calderon-Villalobos LIA, Sharon M, Zheng C, Robinson CV, Estelle M, Zheng N (2007) Mechanismof auxin perception by the TIR1 ubiquitin ligase. Nature 446: 640-645

Tatematsu K, Kumagai S, Muto H, Sato A, Watahiki MK, Harper RM, Liscum E, Yamamoto KT (2004) *MASSUGU2* encodes Aux/IAA19, an auxin-regulated protein that functions together with the transcriptional activator NPH4/ARF7 to regulate differential growth responses of hypocotyl and formation of lateral roots in *Arabidopsis thaliana*. Plant

Cell 16: 379-393

Tian C-e, Muto H, Higuchi K, Matamura T, Tatematsu K, Koshiba T, Yamamoto KT (2004) Disruption and overexpression of *auxin response factor 8* gene of *Arabidopsis* affect hypocotyl elongation and root growth habit, indicating its possible involvement in auxin homeostasis in light condition. Plant J 40: 333-343

Tiwari SB, Hagen G, Guilfoyle TJ (2003) The roles of auxin response factor domains in auxin-responsive transcription. Plant Cell 15: 533-543

Watahiki MK, Yamamoto KT (1997) The *massugu1* mutation of Arabidopsis identified with failure of auxin-induced growth curvature of hypocotyl confers auxin insensitivity to hypocotyl and leaf. Plant Physiol 115: 419-426

Wilmoth JC, Wang S, Tiwari SB, Joshi AD, Hagen G, Guilfoyle TJ, Alonso JM, Ecker JR, Reed JW (2005) NPH4/ARF7 and ARF19 promote leaf expansion and auxin-induced lateral root formation. Plant Journal 43: 118-130

Wu M-F, Tian Q, Reed JW (2006) *Arabidopsis microRNA167* controls patterns of *ARF6* and *ARF8* expression, and regulates both female and male reproduction. Development 133: 4211-4218

Supporting Information

Additional Supporting Information may be found in the online version of this article:

Appendix S1 Relationship between pistil and stamen length in auxin-related mutants.

Figure legends

Fig. 1. Distribution of the number of seeds in one silique in wild type (A), *msg2-1* (B), and hand self-pollinated *msg2-1* (C). One-hundred and five and 129 siliques were examined in wild type and *msg2-1*, respectively. Twenty-six hand pollinations were carried out for *msg2-1* in (C). On average the wild type and *msg2-1* produced 40.0 ± 17.5 and 4.4 ± 7.9 seeds in a silique, respectively, and 46.4 ± 5.9 seeds were present in a silique of hand self-pollinated *msg2-1*. Siliques were examined in 7-week-old plants grown under continuous white light.

Fig. 2. Growth of pistils and stamens in the wild type (Col) and *msg2-1*. (A) Photographs of wild-type and *msg2-1* flowers in flower stages later than 12. A few sepals and petals were removed from flowers or flower buds. Scale bar: 1 mm. (B) Relationship between pistil length and stamen length in the wild type (left) and *msg2-1* (right). (Top and middle) Length of the long (top) and the short stamens (middle) is plotted as a function of length of the pistil in each flower. A thin line is drawn in each panel, having a slope of 45° and passing through the origin. Thus, stamens longer than the pistil in each flower are located above this line. (Bottom) Distribution of pistil length. Stamen and pistil lengths were measured in each flower whose pistil was longer than 1.0 mm. Flowers were obtained from the primary inflorescence of ~7-week-old plants. Of 253 wild-type flowers examined, four were excluded from this figure since their pistils were longer than 3.5

mm.

Fig. 3. Distributions of stamen length in long (top) and short (bottom) stamens in the wild type (Col) (grey bars) and *msg2-1* (bars drawn with bold lines). All stamens longer than 0.7 mm were measured. Data of Figs. 2 and 3 were obtained from the same population of flowers. For more details, see the legend to Fig. 2.

Fig. 4. Time course of growth (top and middle) and growth rate (bottom) of pistils (circle) and long stamens (triangle) in the wild type (Col) (left) and *msg2-1* (right) calculated from histogram of length of pistils (Fig. 2B, bottom) and the long stamens (Fig. 3, top), relationship between pistil and stamen length (Fig. 2B, top), and a measured reference growth rate of pistils. Growth curves are shown in a linear (top) and logarithmic scale (middle). In the middle panel, exponential regression lines are also shown. The regression line for the wild-type pistil growth: length = 0.9985exp(0.01387t) for $0 < t < 69.1$ h (correlation coefficient $R^2 = 0.9958$). The regression lines for the wild-type stamen growth: length = 0.6829exp(0.01567t) for $0.7 < t < 34.7$ h ($R^2 = 0.9957$); length = 0.1612exp(0.05661t) for $38.1 < t < 42.6$ h ($R^2 = 0.9874$); and length = 1.4603exp(0.006609t) for $48.5 < t < 75.1$ h ($R^2 = 0.9951$). The regression line for the *msg2-1* pistil growth: length = 1.0605exp(0.01308t) for $0 < t < 76.6$ h ($R^2 = 0.9955$). The regression lines for the *msg2-1* stamen growth: length = 0.6430exp(0.01552t) for $5.7 < t < 39.4$ h ($R^2 = 0.9975$); length = 0.1532exp(0.04788t) for $46.1 < t < 51.6$ h ($R^2 = 0.9725$); and length = 1.2540exp(0.008244t) for $56.7 < t < 78.6$ h ($R^2 =$

0.9986).

Fig. 5. Expression of *MSG2* promoter::*GUS* (*pMSG2::GUS*) and *DR5::GUS*. (A) Upper part of an inflorescence stained for *pMSG2::GUS*. Flower developmental stage is indicated for flowers or flower buds at stages 11 and later. Scale bar: 2 mm. (B) GUS-stained flowers of *pMSG2::GUS*. 1: early stage 12; 2: late stage 12; 3: stage 13; 4: stage 14; 5: stage 15; 6: early stage 16. Scale bar: 1 mm. (C) GUS activity as a function of length of the long stamens in *pMSG2::GUS* (top) and *DR5::GUS* (bottom). For *pMSG2::GUS*, intensity of blue color was measured in filaments of all the long stamens longer than 0.4 mm. Flowers were treated with (blue solid circles) or without (black open circles) 50 μM NAA for 2 h before fixation and GUS staining. Measured stamens are classified according to their length with a class interval of 0.1 mm. Mean and the standard deviation of color intensity in each class are compared between the NAA-treated and untreated stamens, and blue asterisks are shown when a significant difference ($P < 0.05$; *t*-test) was observed between them. We measured 270 NAA-treated filaments and 295 untreated filaments. For *DR5::GUS*, color intensity was measured in 571 anthers regardless of the long and short stamens. Brown circles show intensity of blue color when flowers were stained in the absence of the GUS substrate, thus indicating the background level of color intensity.

Fig.6. Expression of *MSG2* in different stages of flower as determined by quantitative RT-PCR. *MSG2* mRNA level was examined relative to the

level of *ACTIN2* mRNA. Total RNA was prepared from whole flowers without pedicels. The data indicate the mean and SD of 3 - 6 independently prepared RNA samples. Because the *msg2-1* stamens did not extend over the pistils, stages 14 and 15 were not separable from each other in this mutant. Thus, *msg2-1* flowers were tentatively classified as stage 14 when their long stamens were between 2.0 and 2.5 mm long. Relative mRNA levels of stage 13 and 14 flowers indicated by asterisks are significantly higher than those of stage 12 flowers in each genotype ($P < 0.05$; *t*-test).

Fig. 7. Number of cells in epidermal cell files of stamen filaments. (A) Relationship between stamen length and the number of cells in epidermal cell files of the long (circles) and short (triangles) stamen filaments in the wild type (closed symbols) and *msg2-1* (open symbols). (B) Mean number of cells per cell file in the epidermis of stamen filaments. (C) A short stamen of the wild type. The epidermal cells in one of the cell files are indicated by broken lines.

Fig. 8. Relationship between pistil and stamen lengths in *axr1-12* (A), *axr3-1* (B), *arf6-101* (C), *arf8-1* (D), Ws (E) and *arf19-1 nph4-1* (F). (Top and middle) Length of the long (top) and the short stamen (middle) is plotted as a function of length of the pistil in each flower. (Bottom) Distribution of pistil length. *arf6-101* and *arf8-1* are Ws background; the others are Col background. For more details, see the legend to Fig. 2.

Supplemental Fig. 1. Relationship between pistil and stamen length in

axr2-1, *slr-1*, *pin3-4*, *nph4-1*, *arf19-1*, and *msg2-21*. *msg2-21* is Ws background, while the other mutants are Col background. (Top and middle) Length of the long (top) and the short stamens (middle) is plotted as a function of length of the pistil in each flower. (Bottom) Distribution of pistil length. Stamen and pistil lengths were measured in each flower whose pistil was longer than 1.0 mm. Flowers were obtained from the primary inflorescence of ~7-week-old plants. Of 226 *pin3-4* flowers examined, two were excluded from this figure since their pistils were longer than 3.5 mm. Similarly data of two flowers were excluded out of 85 *msg2-21* flowers.

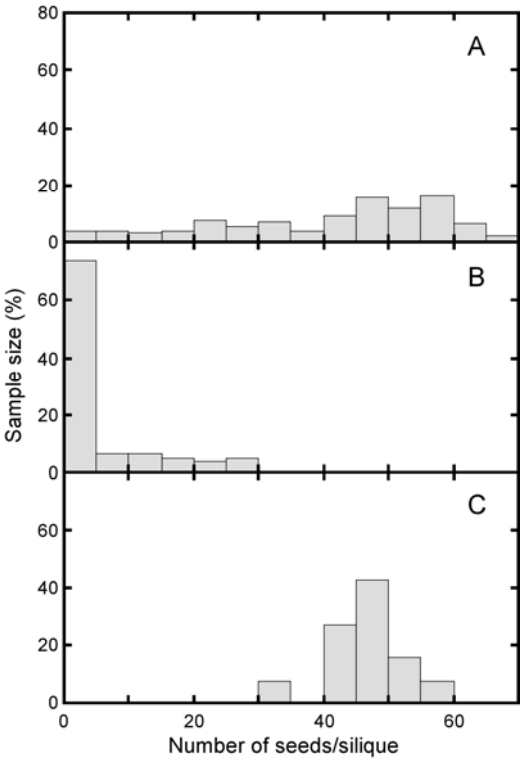

Fig. 1

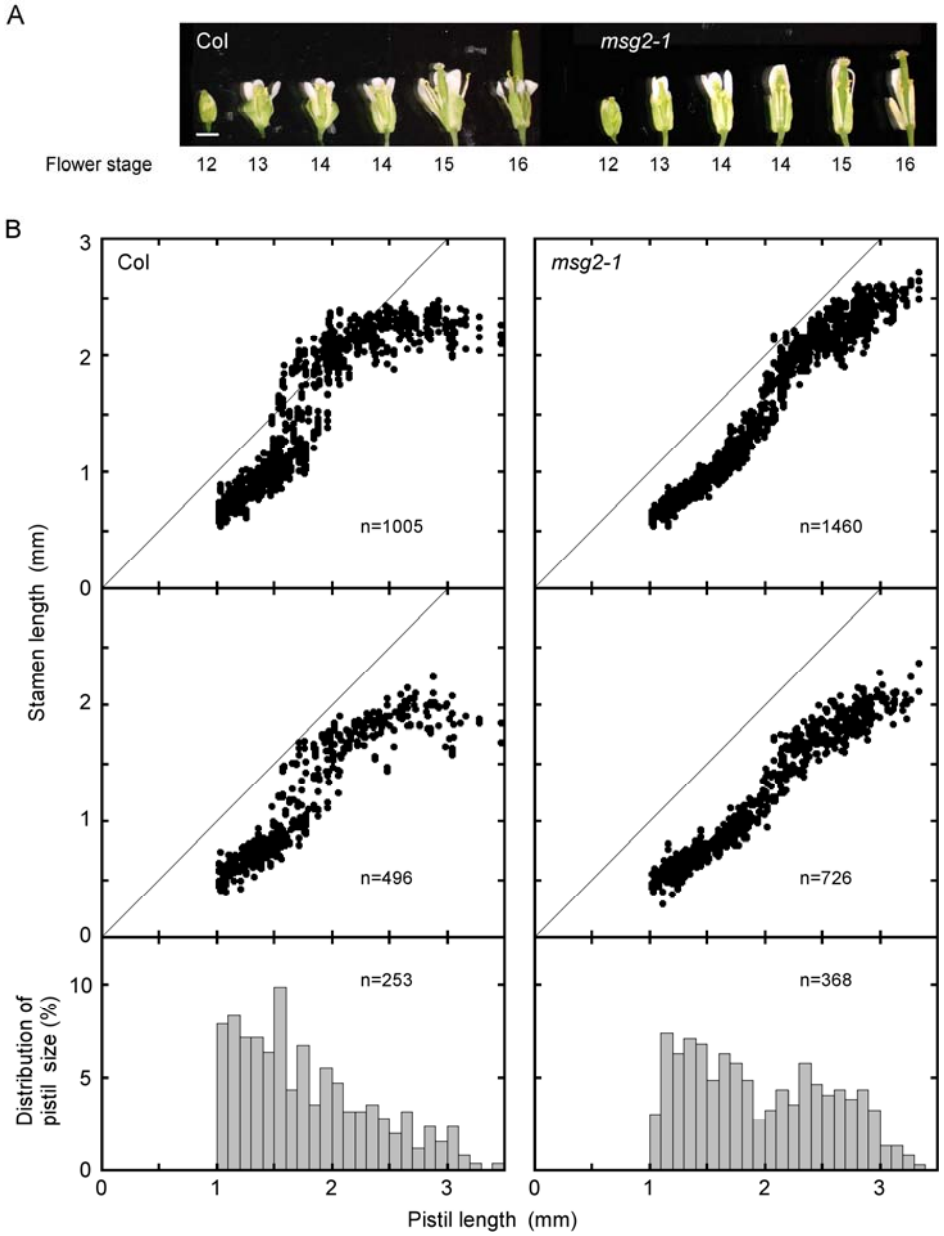
A
Col
msg2-1
Flower stage
12 13 14 14 15 16 12 13 14 14 15 16
B
Col
msg2-1
n=1005
n=1460
n=496
n=726
n=253
n=368
Stamen length (mm)
Distribution of pistil size (%)
Pistil length (mm)

Fig. 2

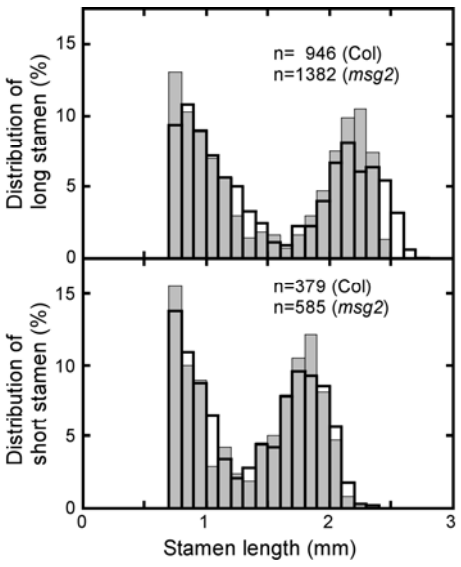
n= 946 (Col)
n=1382 (msg2)
Distribution of long stamen (%)
n=379 (Col)
n=585 (msg2)
Distribution of short stamen (%)
Stamen length (mm)

Fig. 3

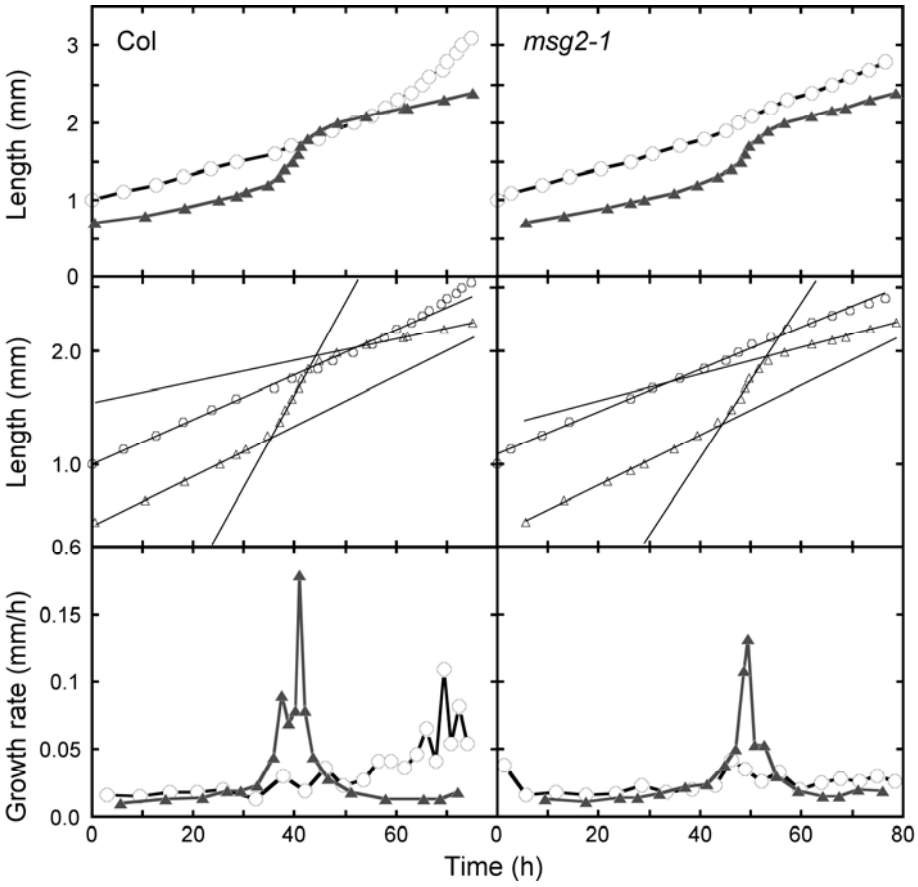
Col
msg2-1
Length (mm)
Length (mm)
Growth rate (mm/h)
Time (h)

Fig. 4

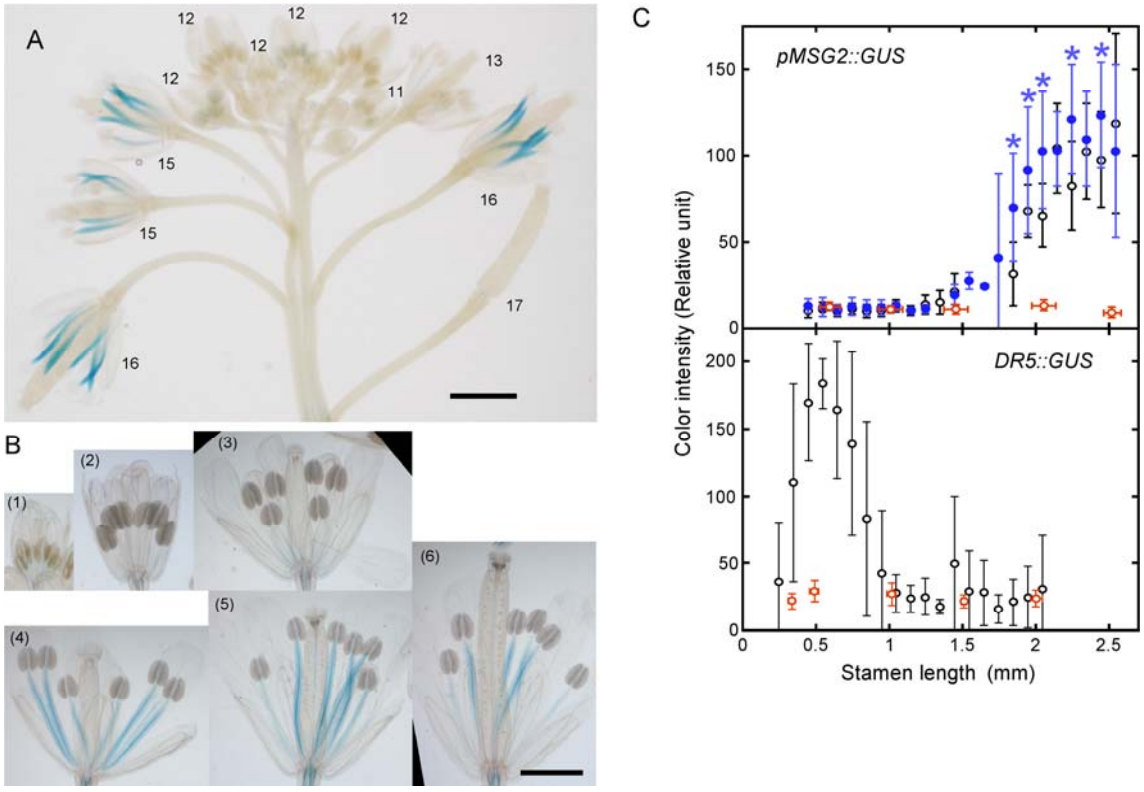
A
12
12
12
12
12
13
11
15
16
15
17
16
B
(1)
(2)
(3)
(4)
(5)
(6)
C
pMSG2::GUS
DR5::GUS
Color intensity (Relative unit)
Stamen length (mm)
0
50
100
150
200
0.5
1
1.5
2
2.5

Fig. 5

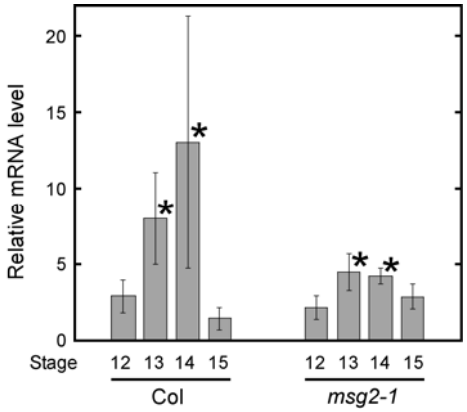
Relative mRNA level
0
5
10
15
20
Stage
12 13 14 15
12 13 14 15
Col
msg2-1

Fig. 6

A

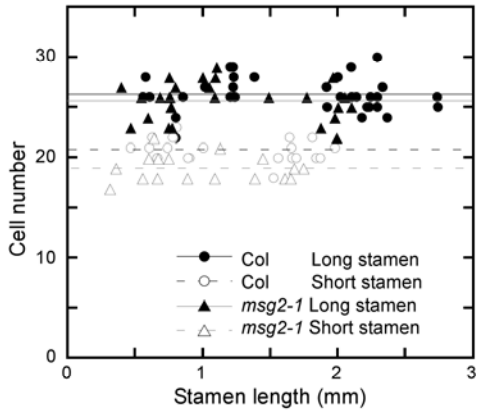

B

		Cell number ± SD
Col	long stamen	26.3±1.7
	short stamen	20.8±1.1
msg2-1	long stamen	25.6±1.8
	short stamen	19.0±1.3

C

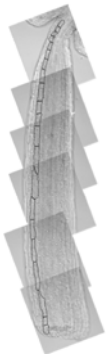

Fig. 7

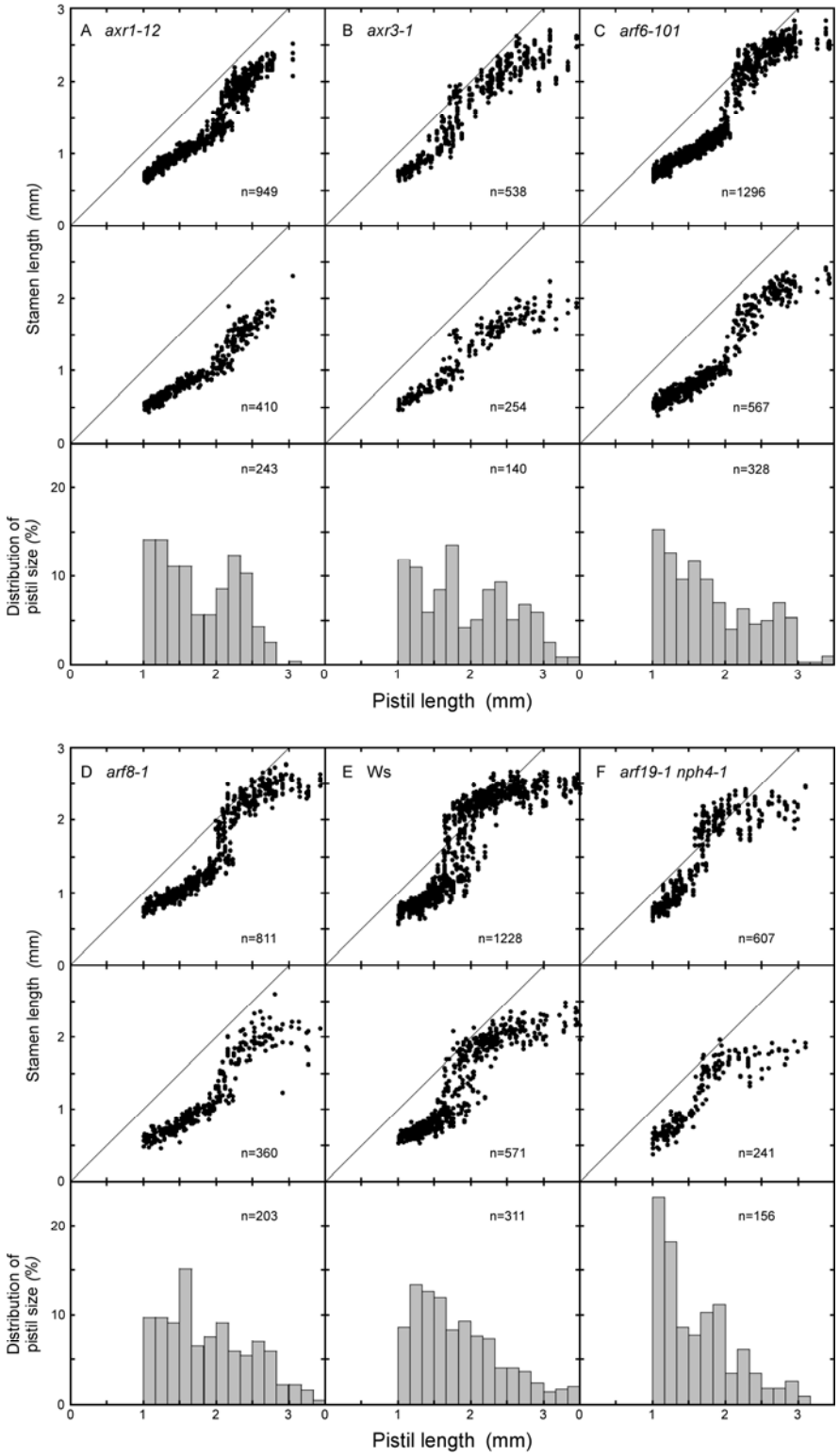
A axr1-12
B axr3-1
C arf6-101
D arf8-1
E Ws
F arf19-1 nph4-1
n=949
n=538
n=1296
n=410
n=254
n=567
n=243
n=140
n=328
n=811
n=1228
n=607
n=360
n=571
n=241
n=203
n=311
n=156
Stamen length (mm)
Distribution of pistil size (%)
Pistil length (mm)

Fig. 8

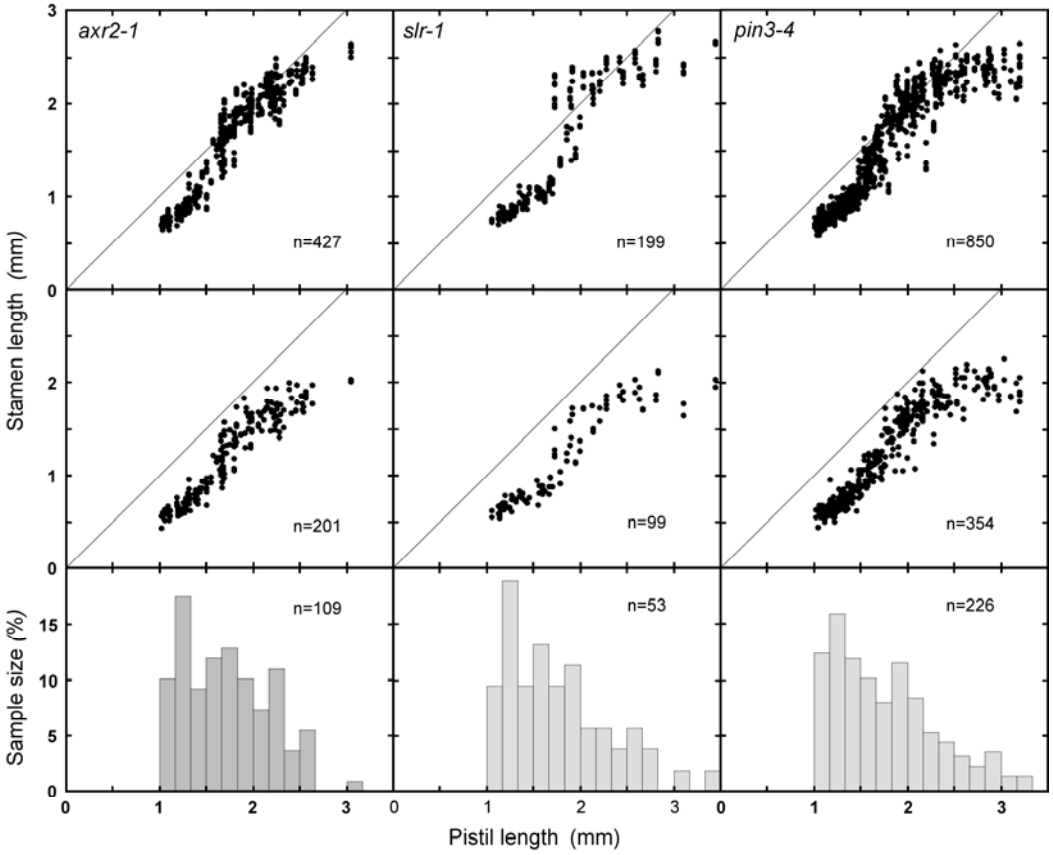
axr2-1
slr-1
pin3-4
n=427
n=199
n=850
n=201
n=99
n=354
n=109
n=53
n=226
Stamen length (mm)
Sample size (%)
Pistil length (mm)

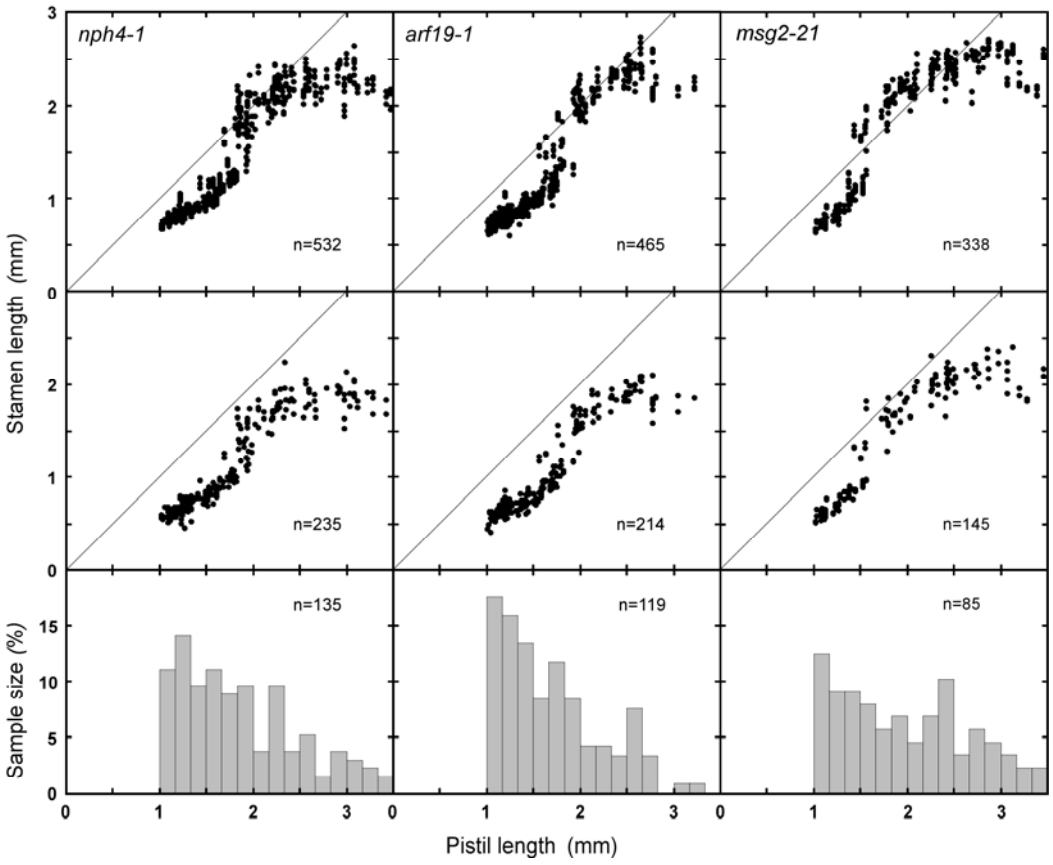
nph4-1
arf19-1
msg2-21
n=532
n=465
n=338
n=235
n=214
n=145
n=135
n=119
n=85
Stamen length (mm)
Sample size (%)
Pistil length (mm)

Suppl. Fig.